Geochemistry Geophysics Geosystems G3
AN ELECTRONIC JOURNAL OF THE EARTH SCIENCES
Published by AGU and the Geochemical Society

Article
Volume 11, Number 2
11 February 2010
Q02Z13, doi:10.1029/2009GC002830
ISSN: 1525-2027

On the mechanism of formation of depositional remanent magnetization

Valeriy Shcherbakov and Natalia Sycheva
Borok Geophysical Observatory, Russian Academy of Sciences, Borok 152742, Russia (shcherb@borok.yar.ru)

[1] Coagulation of particles into aggregates during their settling in an aqueous solution is numerically simulated with regard to Brownian motion, Van der Waals and Stokes's forces, gravitation, and magnetostatic interactions. Clusters obtained have a fractal structure with the average fractal dimension $d = 1.83$. Magnetic grains do not group until their concentration exceeds at least a few percent. The deposition process obeys a scaling principle: the sizes of clusters arriving at the bottom of a basin do not change if the product of the basin depth H and the concentration of initial material c_0 is constant. Attempts at numerical simulations of laboratory redeposition experiments are made. Good agreement between numerical simulations and experimental results by van Vreumingen (1993) demonstrates that the modeling algorithm is based on reasonable physical assumptions. The magnetization of a flocculating suspension is defined by at least seven parameters, which characterize magnetic and nonmagnetic particles, as well as the aqueous medium. This multiparametric dependence hinders estimations of paleofield intensity by the redeposition method because it is practically impossible to reproduce natural conditions in the laboratory. Flocculation influences the magnetization intensity of the settling suspension at concentrations c_0 typical for redeposition experiments or natural sedimentation in lakes and shallow seas. Flocculation is of minor importance for deep oceanic regions because of their extremely low sedimentation rate. However, factors like small-scale turbulence and biotic processes are not taken into account by the model and may require modification of these conclusions. Also, a simple model of pDRM acquisition based on elastic and plastic properties of sediment slurry is proposed.

Components: 11,054 words, 10 figures.

Keywords: sedimentary rocks; flocculation; numerical modeling; clusters; detrital remanent magnetization.

Index Terms: 1540 Geomagnetism and Paleomagnetism: Rock and mineral magnetism.

Received 28 September 2009; **Revised** 8 December 2009; **Accepted** 14 December 2009; **Published** 11 February 2010.

Shcherbakov, V., and N. Sycheva (2010), On the mechanism of formation of depositional remanent magnetization, *Geochem. Geophys. Geosyst.*, *11*, Q02Z13, doi:10.1029/2009GC002830.

Theme: Magnetism From Atomic to Planetary Scales: Physical Principles and Interdisciplinary Applications in Geoscience
Guest Editors: J. Feinberg, F. Florindo, B. Moskowitz, and A. P. Roberts

1. Introduction

[2] Paleomagnetic and rock magnetic studies of sedimentary rocks provide important information on the geomagnetic field history, the magnetostratigraphic time scale, tectonics, paleoclimate and environmental conditions, etc. However, our understanding of the physics of formation of remanent magnetization I_{rd} of sediments is far from being satisfactory. The process of I_{rd} acquisition is evidently related to the process of formation of sediments. The last one consists of the settling of particles through the water column on the water/sediment surface following by gradual compaction and consolidation of the sediment. Accordingly, depositional (DRM) and postdepositional (pDRM) magnetizations were introduced [*Nagata*, 1961].

[3] The first theoretical model of DRM formation was presented by *Nagata* [1961]. The model considers an isolated magnetic spherical particle of a radius r_m settling in water. The viscosity $\eta \approx 10^{-3}$ Pa s of water is the only factor preventing the orientation of its magnetic moment **m** along the direction of an external magnetic field **B**. The angle ϑ between **m** and **B** is determined by the balance between the viscous $8\pi\eta r^3(d\vartheta/dt)$ and magnetic $mB \sin \vartheta$ torques:

$$\frac{d\vartheta}{dt} = \frac{1}{\tau_r}\sin\vartheta, \qquad (1)$$

where the characteristic rotation time of **m** toward **B** is

$$\tau_r = 8\pi\eta r_m^3/mB \approx 6\eta/I_n B. \qquad (2)$$

To derive (2), the relationship $m = I_n v$ is used, where $v = (4\pi/3)r_m^3$ is the volume and I_n is the intensity of natural remanent magnetization (NRM) of the particle.

[4] As follows from (2), even at low $B \approx 50$ μT and $I_n \approx 100$ A/m magnetic particles become aligned along **B** in less than a second [*Stacey*, 1972]. In other words, at any conceivable size of particles I_{rd} should be close to its saturation value I_{sat}. However, in reality remanent magnetization I_{rd} of sediments is usually weaker than any other NRM [*Dunlop and Ozdemir*, 1997] and the relation $I_{rd} \ll I_{sat}$ for field strengths in the range of the Earth's magnetic field is often observed [*Kent*, 1973; *Barton et al.*, 1980; *Tucker*, 1980; *Tauxe and Kent*, 1984].

[5] To solve this problem, thermal fluctuations were suggested as a possible agent to misalign magnetic moments [*Collinson*, 1965; *Stacey*, 1972] but simple calculations show that only a very fine fraction of magnetic grains may be affected by the thermofluctations [*Shcherbakov and Shcherbakova*, 1983; *Dunlop and Ozdemir*, 1997].

[6] As an alternative to the Nagata's model, a flocculation model was proposed by *Shcherbakov and Shcherbakova* [1983] and studied later by *van Vreumingen* [1993], *Katari and Tauxe* [2000], and *Tauxe et al.* [2006]. The idea of the flocculation model is as follows: since each flock contains mainly nonmagnetic grains, its net magnetic moment $\mathbf{m}_{cl}$ only slightly increases with increasing flock size. On the other hand, the viscous torque increases as the cube of the floc size. Thus, one can expect that the flocculation process will increase significantly the alignment time(2) if the particle size r_m is replaced by the floc size. As a cluster sinks to the bottom much more rapidly than an isolated grain, one can therefore assume that its magnetic moment $\mathbf{m}_{cl}$ will not have a sufficient time for its alignment during the settling. Hence, DRM is expected to be far from the saturation which is exactly what the flocculation model tries to explain.

[7] Actually, this reasoning is not completely correct, since it ignores the fact that the magnetic moment of an isolated magnetic particle is already oriented along **B** before the particle enters in a cluster. To understand the problem, two extreme models can be suggested.

[8] 1. The vector **m** of a particle retains its direction after the particle joins a cluster and this tendency is kept at all stages of flocculation. Then the formation of flocs has no effect on the magnetization of a suspension and the DRM formation can be described in terms of the Nagata's model of isolated magnetic particles just with lower rotational diffusion rates.

[9] 2. Collisions to a certain degree randomize the vectors of magnetic moments $\mathbf{m}_{cl}$ of colliding clusters. In other words, grains composing the colliding clusters, may experience random rotations and displacements within the cluster. The randomization of vectors $\mathbf{m}_{cl}$ naturally decreases the net magnetization. Consequently, after each collision the process of aligning of $\mathbf{m}_{cl}$ along **B** starts again. Actually, this assumption constitutes the essence of the flocculation model. Possible reasons for the disorientation of magnetic moments of grains and clusters as a result of collisions will be shortly discussed.

[10] The critical point is: what do experiments tell us about the validity of the Nagata's model? First of all, most of the results concerning redeposition experiments were obtained from measurements of the intensity of remanent magnetization. But the Nagata's model, strictly speaking, describes the magnetization induced in a fluid containing noninteracting individual magnetic grains. Thus, observations of magnetic remanence have only indirect relation to this model and the deduction that the Nagata's model does not fit the experimental data is, in fact, too hasty. Apparently, in order to prove or disprove the validity of the Nagata's model, it is necessary to carry out measurements of magnetization of suspensions in the presence of the external field. Such the experiments first were reported by *Shive* [1985] and *Carter-Stiglitz et al.* [2006] who demonstrated that settling magnetic grains are almost completely aligned along **B** already at B < 100 μT, in accordance with the Nagata's model prediction. However, these experiments were done with pure magnetic suspensions where strong magnetostatic interactions lead to the formation of chains of magnetic particles so one cannot judge the behavior of isolated magnetic grains mixed with nonmagnetic ones. The more detailed and relevant experiments favoring the Nagata's model were reported by *van Vreumingen* [1993] who studied the magnetization of suspension of mixtures of magnetic and nonmagnetic fine grains at different salinities of aqueous solution. As observed, the magnetization intensity of suspensions at relatively small salinities <3 g/*l*, measured in the presence of the external field only 5 s after the start of sedimentation, was at its peak values close to I_{sat}. More evidence supporting the Nagata's model were given by *Johnson et al.* [1948] and *Tauxe et al.* [2006] who showed that in some cases I_{rd} is indeed close to I_{sat} at low B.

[11] Altogether, previous studies found that, laboratory redeposition experiments in fields of order of 100 μT often produce DRM which is far from the saturation [*Kent*, 1973; *Barton et al.*, 1980; *Tucker*, 1980; *Tauxe and Kent*, 1984]. Equally importantly, *van Vreumingen* [1993] found that at high salinities the magnetization of suspensions drastically fall below I_{sat}. All these observations favor the flocculation model.

[12] Thus, in order to understand the formation of DRM, first a detailed analysis of the flocculation process in mixtures of magnetic and nonmagnetic grains should be carried out. This task and a theoretical study of the acquisition of the magnetization of settling flocculating suspensions containing magnetic grains dispersed in a nonmagnetic matrix is the main purpose of this paper. Due to the great complexity of these processes, we restrict ourselves with the case of spherical settling grains. Also, we will avoid problems related to the hydrodynamic torques developing during the settling and flocculation of grains. Attempts to treat this difficult topic are presented by *Chermous and Shcherbakov* [1980], *Heslop* [2007], and *Mitra and Tauxe* [2009]. Finally, no chemical and biological processes will be taken into account though we fully appreciate that their role also can be critical. So, our calculations were designed, first of all, to explain data obtained in laboratory redeposition experiments which are usually carried out under well known restricted conditions. Due to these restrictions, some conclusions of this study may not capture all aspects of flocculation but we believe that on this stage of our knowledge of the processes of the formation of DRM and pDRM even the restricted analysis suggested here can bring new and valuable results.

2. Numerical Modeling of Flocculation

[13] Agglomeration of colliding particles is ensured by the Van der Waals forces, though magnetic particles can be additionally affected by magnetic forces. To avoid a misunderstanding, note that except for the agglomeration, collisions may cause also breakup of clusters. However, to simplify the task, we ignore in this paper the process of dissociation of clusters. Besides, colliding clusters may not necessary merge together but their unification may happen with some probability β only. Again, for the sake of simplicity we suggest in the further calculations that the collisions are highly effective, so $\beta = 1$. The opposite case $\beta \ll 1$ will be discussed later.

[14] One should discriminate between thermal and kinematic coagulation. In the first case, particles collide due to their Brownian motion. In the second case, it happens due to their directional motion external forces. Gravitational coagulation, when large particles pick up fine grains settling more slowly, is one of the variants of kinematic coagulation.

[15] According to *Fuchs* [1964], the rate of thermal coagulation of two particles of radii r and R in a pair due to the Brownian motion is

$$\gamma_{br} = \frac{2k_B T (r+R)^2}{3\eta r R}. \quad (3)$$

Here k_B is Boltzmann's constant, T is temperature. The characteristic time for formation of a pair of particles is $\tau_{br} = 1/(\gamma_{br} n)$, where n is the concentration of particles (number per unit volume) in the suspension.

[16] For the gravitational coagulation, consider a particle of the radius R settling at the Stokes's velocity $u(R) = 2\Delta\rho g R^2/9\eta$ through a layer of particles of the radius r and density $n(r)$ that move at the velocity $u(r)$. Here $\Delta\rho = \rho_s - \rho_w$, where ρ_s is the density of settling grains, ρ_w is the density of water, g is the gravity acceleration. From simple geometrical consideration the rate of gravitational coagulation can be found as [*Shcherbakov and Shcherbakova*, 1983]

$$\gamma_{gr} = \pi(R + r)^2 |u(R) - u(r)|. \quad (4)$$

The first numerical scheme to study the properties of clusters forming in the process of Brownian motion was the so-called Diffusion Limited Aggregation (DLA) particle–cluster model [*Witten and Sander*, 1981]. To start the modeling, a spherical particle of a radius r was placed at the center of the sphere of a radius $R_0 \gg r$. Then an identical particle was generated on the surface of the embracing sphere and starts to move due to the Brownian motion until it collides with the central grain. If the random walking led a particle outside the sphere, another particle was generated on the surface of the sphere and the whole procedure started again. This process continues as long as the number of particles composing the cluster in the center achieves a given number N. The Brownian motion was simulated as a random movement with an amplitude $\sigma = \sqrt{kT/(3\pi\eta r)\Delta t}$ along an arbitrary direction. The time interval Δt in this formula is calculated as the time at which the amplitude σ is equal to the particle's radius r. The DLA model is a perfect tool for testing numerical simulations as the fractal dimension of the clusters generated by means of this model is known to be exactly $d = 2.5$. With our program, we obtained $d = 2.44 \pm 0.13$, which meets this requirement.

[17] In a more complex cluster–cluster aggregation (CCA) model [*Meakin*, 1983; *Kolb et al.*, 1983], all N particles of the radius r are initially randomly distributed inside a cube with a certain relative volume concentration of grains c. Then all grains simultaneously start Brownian motion and clusters are generated due to the collisions. The clusters also experience Brownian motion and eventually unite into larger clusters. To avoid particles from moving outside the initial cube, periodic conditions were applied on its surfaces. In other words, if a grain intersects a face of the cube, it appears on the opposite face. Brownian motion of clusters is simulated in the same way as in the DLA model, but the particle size r is replaced by the so-called gyration radius $R_g = \sqrt{\frac{1}{n}\sum_{i=1}^{n}(\mathbf{r}_i - \mathbf{r}_c)^2}$ characterizing the cluster size. Here $\mathbf{r}_c$ is the radius vector of the center of mass of the cluster, n is the number of particles in the cluster, $\mathbf{r}_i$ is the radius vector of the ith particle in the given cluster.

[18] Results of calculations in CCA model differ significantly from those obtained in the DLA model. Clusters resulting from random aggregation of smaller clusters with different numbers of particles are less dense and more irregular (Figure 1). In some cases the structure of the final cluster is so bizarre that its fractal dimension could not be calculated. The calculated average fractal dimension for the CCA model (when it could be calculated) is $d = 1.83 \pm 0.23$ which is significantly lower than d for the DLA model and agrees with the results reported by *Meakin and Jullien* [1988].

[19] The specificity of our task demands that apart from Brownian motion and Van der Waals forces, we must account for the gravitational $\mathbf{F}_{gr} = \Delta\rho v\mathbf{g}$, magnetostatic interaction $\mathbf{F}_{ms}$ and Stokes's friction $6\pi\eta\mathbf{u}$ forces. For a single particle the balance of these forces is $\mathbf{F}_{gr} + \mathbf{F}_{ms} = 6\pi\eta r\mathbf{u}$. Here $\mathbf{u}$ is the vector of velocity of the particle. The same expression can be applied to a cluster, with r being replaced by the gyration radius R_g. The settling velocity of a cluster (neglecting the magnetostatic forces) is $u(R_g) = (\Delta\rho g\sum_{i=1}^{n} v_i/6\pi\eta R_g)$. Let r be the characteristic radius of particles composing the cluster, then $v_i = (4\pi/3)r^3$ and $u(R_g) = 2\Delta\rho g n r^3/9\eta R_g$. As far as $n \approx (R_g/r)^d$, we obtain

$$u(R_g) = 2\Delta\rho g r^2 (R_g/r)^{d-1}/9\eta. \quad (5)$$

From (5) $u \propto R_g^{d-1} \propto R_g^{0.83}$ At $d = 1.83$ (CCA model) this dependence is very close to the empirical relationship $u \propto R_g^{0.78}$ used by *Katari and Tauxe* [2000] and *Tauxe et al.* [2006] in their studies of the flocculation model.

[20] The magnetostatic interaction force is $\mathbf{F}^i_{ms} = -grad[\mathbf{m}_i(\mathbf{B} + \mathbf{B}^i_{int})]$, where $\mathbf{B}^i_{int}$ is the interaction field. For the dipole–dipole approximation $\mathbf{B}^i_{int} = \sum_{j\neq i}^{N_m} \frac{3(\mathbf{m}_j \cdot \mathbf{r}_{ij})\mathbf{r}_{ij}}{r_{ij}^5} - \frac{\mathbf{m}_j}{r_{ij}^3}$, where the summation is done over magnetic grains, N_m is the number of magnetic

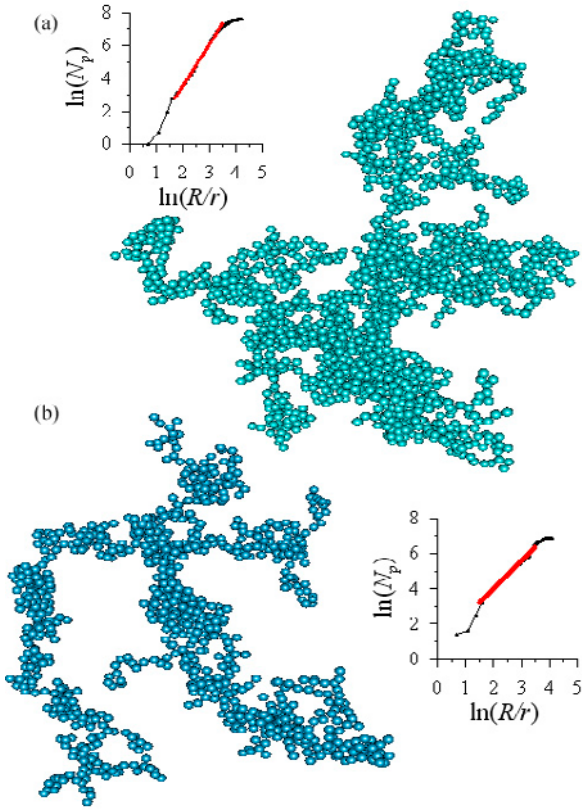

Figure 1. Computer modeling of the flocculation process. Configuration of clusters in the CCA model with regard for Brownian motion and Van der Waals forces, $c = 0.1\%$. (a) $N = 2000$ and $r = 0.3$ μm. (b) $N = 1000$ and $r = 0.3$ μm. For each case the log-log dependence of the number of particles N_p inside a sphere of radius R as a function of the normalized distance R/r from the center of mass of the cluster is shown in the insets. The slope of the linear segment of these curves (red lines) yields the fractal dimensions $d = 2.44$ (Figure 1a) and 1.57 (Figure 1b).

particles and r_{ij} is the distance between the ith and jth particles. For simplicity, a cluster was also considered as a magnetic dipole with the magnetic moment $\mathbf{m}_{cl} = \sum_{i=1}^{n_m} \mathbf{m}_i$, where n_m is the number of magnetic particles in the cluster.

[21] Magnetic moments of free particles vary with time due to the thermofluctations. To simplify the task, the mean field approximation was used, when $\mathbf{m}_i = m_i \mathbf{b}_i L[m_i(B + B^i_{\text{int}})/k_B T]$, where $\mathbf{b}i$ is the unit vector along the direction $\mathbf{B} + \mathbf{B}^i_{\text{int}}$, $L(x)$ is the Langevin function.

[22] Modeling of the deposition process with regard to the magnetostatic and gravitation forces was performed by calculating the forces and corresponding velocities of each object in each time interval Δt. Until the next updating, grains and clusters moved linearly at the calculated velocity $\mathbf{u}^i$. At the next updating, they were randomly displaced in accordance with the CCA scheme described above. These calculations yielded the fractal dimension $d = 1.81 \pm 0.31$, which only insignificantly differs from the result obtained for the original CCA model without gravitation and magnetostatic terms.

[23] One could expect that the magnetostatic interactions at a high concentration c_m of magnetic particles would lead to formation of groups containing predominantly magnetic particles. According to *Fuchs* [1964], the rate of agglomeration γ_{br} of magnetic particles is increased by $\Gamma \approx (m^2/r_m^3 kT)^{1/3} = (16\pi^2 I^2 r_m^3/9kT)^{1/3}$ times in comparison with the rate of agglomeration of the nonmagnetic ones. Indeed, due to the long-range nature of magnetic forces, when the distance between two magnetic particles becomes sufficiently small, the energy of their mutual magnetostatic interaction exceeds the thermal one, favoring their collision. The critical distance r_{ms} is determined by the condition $m^2/r_{ms}^3 = kT$. Assuming $R \approx r$, the formula (3) simplifies to $\gamma_{br} \approx 8k_B T/3\eta$. On the other hand, the critical radius r_{ms} is certainly $\gg r_m$ if the magnetostatic interactions are strong enough to influence the collision rate. But at $R \gg r$, the rate (3) reduces to $\gamma_{br} \approx 2k_B TR/3\eta r$. Replacing here R by r_{ms} we obtain (by the order of value) the estimate for Γ given above. The characteristic time of forming a pair of particles is $\tau_{br} = 1/(\gamma_{br} n)$, and the rate of agglomeration of only magnetic fraction can be estimated as $\Gamma/(\gamma_{br} n c_m)$. Hence, it would prevail over the nonmagnetic grain collision rate at $c_m > 1/\Gamma$. To estimate Γ numerically, note that $\Gamma \approx 20$ for single-domain (SD) magnetite grains with the radius $r \approx 50$ nm. Approximately the same value of Γ holds for pseudo-single-domain grains with $r_m \approx 500$ nm and $I_n \sim 10$ kA/m. Thus, the formation of a pair of magnetic particles is more probable than the formation of a pair containing both magnetic and nonmagnetic particles, if c_m exceeds at least a few percent.

[24] To verify this suggestion, we modeled numerically the coagulation of mixture of 1950 nonmagnetic and 50 magnetite particles with $r = r_m = 0.1$ μm, $I_n = 485$ kA/m, total volume concentration of solid phase $c = 0.1\%$. First, the grains were randomly distributed over the cube with total volume concentration of solid phase $c = 0.1\%$. Next, they were allowed to move under the action of Brownian motion, Van der Waals forces, Stokes settling velocity, and magnetostatic interactions. Again, the

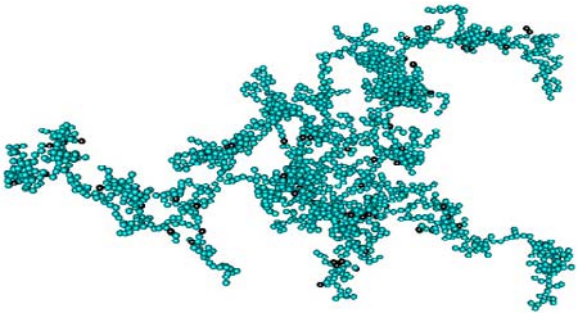

Figure 2. Computer modeling of the flocculation process in the CCA model, including Brownian motion, Van der Waals forces, Stokes settling velocity, and magnetostatic interactions: $N = 2000$, $r = 0.1$ μm, $c = 0.1\%$, and the number of magnetic particles (colored black) is $0.05N$. White small patterns on the grains in Figures 2 and 3 are imaginary light spots to highlight the three-dimensional structure of the cluster. Data are from *Shcherbakov and Sycheva* [2008].

periodic conditions were applied on the cubic faces. Almost no agglomeration of magnetic particles is seen in the final cluster (Figure 2). Further calculations showed that magnetic particles do agglomerate only at high enough concentrations $c_m > 10\%$. However, even then only small groups consisting of a few magnetic particles are seen (Figure 3). Note that among these groups no chains form but instead the agglomerates of magnetic grains form bundle like structures. This result provides an argument in favor of the suggestion that chains of magnetite particles, which are observed sometimes in sediments, are of biogenic origin as big concentrations of the magnetic fraction are very rare in the sedimentary rocks.

[25] Next, modeling of deposition of continuously supplied sedimentary material was carried out. For the beginning, 200 particles with initial volume concentration $c = 0.1\%$ were uniformly distributed over the top cubic part of a narrow long parallelepiped with width A and height $A^* \gg A$ while the rest volume of the parallelepiped was empty. Then the particles were allowed to move under the combined action of the Brownian motion, Van der Waals forces and Stokes settling velocity. Magnetostatic interactions were neglected on the basis of the previous numerical experiments. This time the periodic conditions were set only on the walls of the parallelepiped as the grains were allowed to settle down throughout the whole parallelepiped. When a grain or cluster crossed the bottom of the top cube, the same amount of grains appeared on the top face of the parallelepiped to mimic grain by grain deposition. The particles (or the clusters) which reached the bottom of the parallelepiped were fixed there. The calculations were stopped at the moment when 15000 particles dropped. Figure 4a demonstrates the distribution of grains in the top cubic part of the parallelepiped (that is near its top face) where the grains are yet rarely united in pairs or clusters. In contrast, near the bottom the vast majority of particles are agglomerated into clusters which contain tens and even hundreds of particles (Figure 4c).

3. Analytical Description

[26] Assume for simplicity that clusters consist of identical particles of the same size r. As it was shown that the magnetostatic interactions are insignificant at realistic concentration of the magnetic fraction, below we will neglect their role in the flocculation. The agglomeration of particles and aggregates due to Brownian motion can be described by the Smoluchowski coagulation equation. The details of calculation are presented in Appendix A.

[27] Figures 5 and 6 show how the exponential d.f. $f(n, 0) = \exp(-n)$ transforms with the dimensionless depth $X = \frac{3c_0 x}{4r}$ to a nonmonotonic d.f with a maximum at a certain n. Here c_0 is the relative volume concentration of material on the basin surface. The accuracy of the solution was checked by monitoring the invariant U, which during the calculations changed by not more than 0.3% of its initial value. For convenience, the fractal dimension d

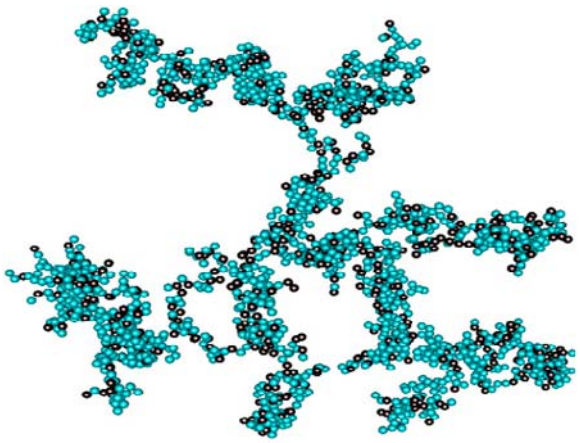

Figure 3. Computer modeling of the flocculation process at high concentration of the magnetic phase. Results of calculations of the CCA model, including Brownian motion, Van der Waals forces, Stokes settling velocity, and magnetostatic interactions: $N = 2000$, $r = 0.1$ μm, $c = 0.1\%$, and the number of magnetic particles (colored black) is $0.3N$.

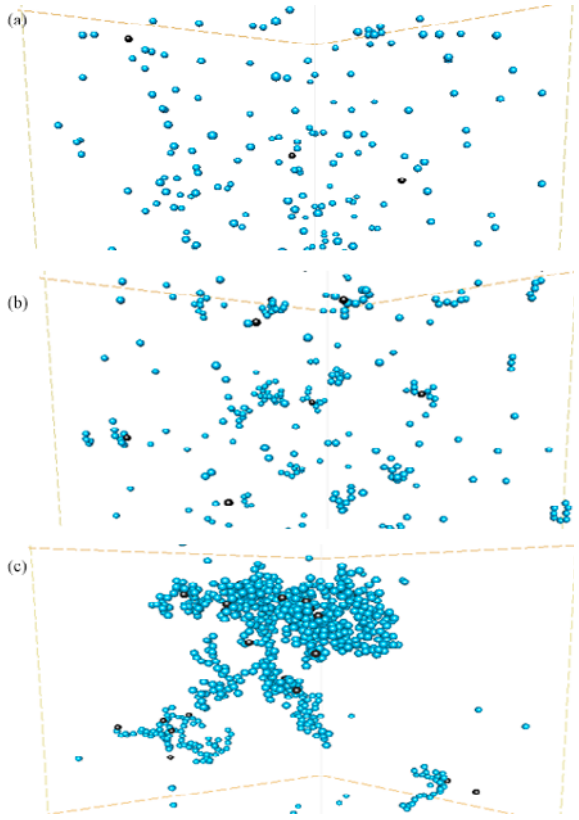

Figure 4. Results of modeling of the deposition of continuously supplied sedimentary material in the parallelepiped with width A = 94 μm and height A^* = 1.41 cm following the CCA model. r = 1.0 μm, and c = 0.1%. (a) Configuration near the water surface, (b) configuration in the middle of the parallelepiped at a depth of 0.5 cm, and (c) configuration at a depth of 0.95 cm. The big cluster in Figure 4c consists of 516 particles with d = 2.4.

was set equal to 2, which differs insignificantly from its average value d = 1.83 obtained by the numerical simulations described above. The dependence of the average number of grains $\overline{n}$ in clusters on X is shown in the insets to Figures 5 and 6. For comparison, the dependence $\overline{n}(X)$ obtained by numerical modeling as described in section 4, is also shown in Figure 5. As expected, this curve strongly fluctuates with depth due to insignificant statistics but the similarity between the red and blue and lines is clearly seen proving the general identity of the analytical and numerical approaches.

[28] The average number of particles in clusters $\overline{n}(X) = \int nf(n, X)dn/\int f(n, X)dn$ is shown in the inset by solid line. As expected, $\overline{n}(X)$ increases with X. For comparison, the average number of particles

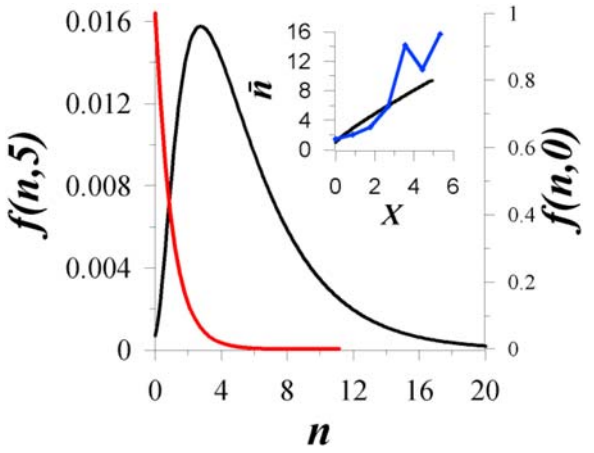

Figure 5. Results of numerical solution of the Smoluchowski coagulation equation (A6) for $f(n, X)$ for r = 0.5 μm and X = 5 (black line). The initial distribution function $f(n, 0) = \exp(-n)$ (red line). The dependence $\overline{n}(X)$ is shown in the inset by the black line. The blue line in the inset is the result of numerical modeling in terms of the CCA model. Data are from *Shcherbakov and Sycheva* [2009].

in clusters as a function of depth (blue line) was computed by the same numerical algorithm as it was used to compute Figure 4. As expected, for the numerical modeling $\overline{n}(X)$ strongly fluctuates with depth but the similarity between the two curves is kept.

[29] Figure 6 is constructed for the case of coarse particles with the radius r = 3 μm. As is seen, the

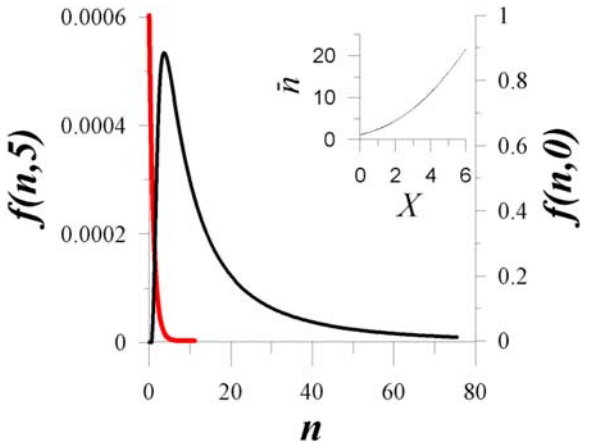

Figure 6. Results of numerical solution of the Smoluchowski coagulation equation (A6) for $f(n, X)$ for r = 3 μm and X = 5 (black line). The initial distribution function $f(n, 0) = \exp(-n)$ (red line). The dependence $\overline{n}(X)$ is shown in the inset by the black line. Data are from *Shcherbakov and Sycheva* [2009].

average size of clusters rises appreciably faster now being close to a parabolic law (inset in Figure 6):

$$\overline{n}(X) = 1.3 + 0.7X + 0.45X^2. \quad (6)$$

This phenomenon is accounted for by the predominance of the gravitational type of coagulation for coarse grains, when the association constant $s(n, k)$ sharply increases with increasing n and k, that is, with cluster sizes.

4. Scaling Law

[30] The invariant (A5) can be reshaped as

$$\frac{4\pi r^3}{3}\int_0^\infty u(n)nf(n,x)dn = \overline{u}\frac{4\pi r^3}{3}\int_0^\infty nf(n,x)dn$$
$$= \overline{u}(x)c(x) = const, \quad (7)$$

where $\overline{u}(x)$ is a characteristic velocity, $c(x)$ ix the concentration of the solid phase at a given depth x. On the basin surface $\overline{u}(0) = u_0$ where $u_0 = 2\Delta\rho g r^2/9\eta$ is the velocity of individual settling grains, $c(0) = c_0$. On the bottom $\overline{u} = u_{dep}$, $c = c_b$, where the deposition rate u_{dep} varies from $\sim 10^{-8}$ cm/s in lakes to $\sim 10^{-11}$ cm/s in pelagic zones of oceans. The relative volume concentration of the solid fraction on the sediment/water interface is $c_b \approx 0.05$. Using these definitions, the following relationship can be inferred from (7)

$$c_b/c_0 \approx u_0/u_{dep}. \quad (8)$$

Taking for certainty $r \sim 1$ μm, we can estimate from (8) $c_0 \sim 10^{-6}$ for lakes and $c_0 \sim 10^{-9}$ for oceanic regions.

[31] As follows from (A8), the dimensionless depth X does not change if the basin depth H and the surface concentration c_0 of the initial material vary in such the way that the product

$$Hc_0 = \text{const}. \quad (9)$$

In other words, the deposition process obeys a scaling principle: the d.f. $f(n, x)$ is invariant when H and c_0 vary in accordance to (9). Physically, this property follows from the fact that the efficiency of coagulation is directly proportional to the concentration c_0 of particles in the surface layer. Evidently, this circumstance must be taken into account in redeposition experiments because of the validity of (9) is a necessary (but not sufficient!) condition for the similarity between the deposition processes taking place in situ and in laboratory conditions.

[32] Regarding the practical significance of the scaling law, note that redeposition experiments often use different protocol of settling regime as compared with the settling process in nature. Indeed, in nature the deposition takes place continuously, while most redeposition experiments are carried out by adding discrete portions of sediments. This way of deposition leads to the well-known phenomenon of layering of the settled sediment into coarse and fine fractions. Thus, it cannot mimic the distribution function of sizes of flocs in natural sediments. Hence, if a laboratory redeposition experiment is aimed to imitate the natural deposition process, it should be performed by continuous method. At least, the portions must be as small and frequent in time as possible.

[33] Denoting the rate of redeposition as u_{red} and assuming that c_b and u_0 are the same for deposition and redeposition processes, the condition (9) with help of (8) becomes

$$\frac{u_{red}}{u_{dep}} = \frac{H}{h}. \quad (10)$$

This relationship can be used as a guide to carry out redeposition experiments. For example, imagine a material taken from a lake with the sedimentation rate u_{dep} = 0.3 mm/yr and the depth H = 100 m. According to (10), the correct redeposition of this material in a vessel with the height h = 10 cm requires the redeposition rate $u_{red} \approx 1$ mm/d. However, it is much more difficult to satisfy (8), if very slow accumulating ocean sediments with $u_{dep} \approx$ (0.1–1) mm per 100 yr are investigated. Simple calculations show that despite the big $H \approx$ (1–5) km, a redeposition experiment should continue at least for a year.

5. Magnetization of Suspension in the Mean Cluster Approximation

[34] To describe the competing processes of orientation and randomization of the magnetic moments of flocs during their settling, let us modify equation (1) by adding a random force generated by the collisions. Then (1) takes a form of a Langevin equation:

$$\frac{d\vartheta}{dt} = -\frac{\sin\vartheta}{\tau_r} + f(t)\delta(t - t_i), \quad (11)$$

where $f(t)$ is the random force, $\{t_i\}$ is the collision time sequence, $\tau_r = 8\pi\eta R_g^3/m_{cl}B$ is the characteristic time of rotation of a cluster obtained by a generalization of (2) for the case of a cluster with the gyration radius R_g. Due to low relative content of magnetic

particles in a suspension, clusters contain mainly nonmagnetic grains, so roughly $m_{cl} \sim m$. Taking into account that $(R_g/r) \approx n^{1/d}$, the expression for τ_r can be written as follows

$$\tau_r = \frac{6\eta n^{3/d}}{I_n B}\left(\frac{r}{r_m}\right)^3, \quad (12)$$

where r denotes the radius of nonmagnetic particles. To solve (20) numerically, let us write it in the finite differences:

$$\vartheta(t_n) = \vartheta(t_{n-1}) - \frac{\sin\vartheta_{n-1}}{\tau_r}\Delta t + f(t), \quad (13)$$

where $\Delta t = t_n - t_{n-1}$. The function $f(t) = 0$, if a collision did not occur in the time interval Δt but $f(t)$ is equal to a random number distributed with equal probability within the range $(-D, D)$ around ϑ_{n-1} if $t_i \in \Delta t$. The parameter D characterizes the intensity of the randomization. Of course, the suggestion of equal probability is a rough approximation to the reality and it is taken for the sake of simplicity only. The probability that a collision took place is $P(\Delta t) = \nu\Delta t$, where ν is the total collision rate determined by the formula

$$\nu(n, X) = \int_0^\infty \gamma(n,k)N(k,X)dk. \quad (14)$$

The presence or absence of a collision corresponds to the inequalities $\nu\Delta t < a$ and $\nu\Delta t > a$, respectively, where a is a random number distributed with equal probability within (0, 1). The value of Δt must satisfy the requirements $\nu\Delta t \ll 1$ and $\Delta t/\tau_r \ll 1$. For numerical modeling, Δt was taken as the smallest one from $\Delta t = 0.1/\nu$ and $\Delta t = 0.1\tau_r$.

[35] The complexity of the problem stems from the fact that τ_r and ν changes with each collision. For this reason, the following simplifications were made. First, the approximation of average cluster was used by replacing n with $\overline{n}$ in (12) and (14). Second, only the gravitational coagulation was taken into account to compute (14). The latter assumption is justified because of this type of coagulation prevails when sizes of particles and clusters exceed 1 μm which is often the case. Then (14) reduces to:

$$\nu(\overline{n}, X) = 2\pi N_0 \Delta\rho g r^4 \gamma/9\eta = \gamma/t_0, \quad (15)$$

where $t_0 = 6\eta/c_0\Delta\rho g r$ is the characteristic time between the collisions and

$$\gamma = \int_0^\infty \left(\overline{n}^{1/d} + k^{1/d}\right)^2 \left|\overline{n}^{(d-1)/d} - k^{(d-1)/d}\right| f(k,X)dk. \quad (16)$$

The integral (15) was calculated using the numerical solution of (A6) for $f(k, X)$ at $a = 0$, that is for the case of only gravitational coagulation when the d. f. $f(k, X)$ is universal and does not depend directly on the characteristics of grains. As occurred, in this approximation γ only slightly changes with X being equal approximately to 1.5. For this reason, we assume in the further calculations that the collision rate does not change with depth.

[36] From (5), the settling velocity of the mean cluster is $u(R_g) = 2\Delta\rho g r^2 (\overline{n})^{(d-1)/d}/9\eta$. Using the definition $u = dx/dt$, with help of (5), (A8) and (6), the following equation for the dependence $X(t)$ for the mean cluster is obtained:

$$t_0 \frac{dX}{dt} = \sqrt{a + bX + cX^2} \quad (17)$$

For the sake of simplicity let us put $d = 2$. Integrating (17), we find

$$X(t) = \frac{b(\cosh(t/t_0) - 1) + 2\sqrt{ac}\sinh(t/t_0)}{2c}. \quad (18)$$

Substituting (18) into (6), the dependence $\overline{n}(t)$ can be found. In turn, the knowledge of this dependence enables us, with the help of (12), to derive $\tau_r(\overline{n}(t))$. Then, following the algorithm described above, one can calculate the curve $\vartheta(\vartheta_0, t)$ from (13) for a particular realization of the random process. Here ϑ_0 is the angle ϑ at $t = 0$. Inverting the transformation (18), the relationship $\vartheta(\vartheta_0, X)$ can be determined.

[37] The magnetization of suspension normalized to I_{sat} is

$$i_{sus}(X) = \int_0^\pi \cos[\vartheta(\vartheta_0, X) f(\vartheta_0) d\vartheta_0, \quad (19)$$

where $f(\vartheta_0)$ is the d.f. of initial angles ϑ_0 on the surface $X = 0$.

[38] Figure 7 illustrates the dependence $i_{sus}(X)$ obtained by averaging 1000 realizations of the random process $\vartheta(\vartheta_0, t)$ with ϑ_0 randomly distributed over the interval $(0, \pi)$. Note that all numerical calculations of the magnetization presented here and below were carried out assuming the intensity of the external field $B = 50$ μT. Value of $I_n = 100$ kA/m is taken to represent small submicron pseudo-single-domain (PSD) grains while the weak magnetization intensity $I_n = 1$ kA/m was chosen to model either magnetically soft multidomain (MD) particles or magnetically weak hematite magnetic fraction, or the case when small SD-PSD grains are attached to nonmagnetic grains of much bigger sizes, say, about 1 μm.

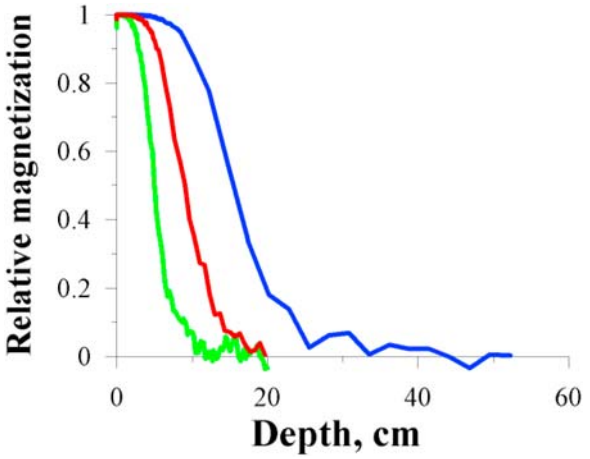

Figure 7. Computer modeling of variations in magnetization of suspension i_{sus} with depth x for $D = \pi$, $c_0 = 0.05\%$, and $r = r_m = 1$ μm. $I_n = 1$ kA/m (green line), $I_n = 10$ kA/m (red line), and $I_n = 100$ kA/m (blue line). Data are from *Shcherbakov and Sycheva* [2009].

[39] As one would expect, the magnetization of the upper layer of suspension very quickly reaches the fully saturated state after the start of settling, while in the deeper layers i_{sus} sharply decreases due to the occurrence of frequent collisions. In the specific examples, presented in Figure 7, this occurs at the depths of a few cm.

[40] The drastic decrease of i_{sus} with X means that the magnetic moments $\mathbf{m}_{cl}$ of clusters undergo almost complete randomization. To find the asymptotic value of i_{sus} at $X \to \infty$, that is at $\nu\tau_r \gg 1$, note that for the entirely random distribution of $\mathbf{m}_{cl}$ over the angles ϑ, the d. f. $f(\vartheta) = \sin\vartheta$. The presence of a weak magnetic field disturbs $f(\vartheta)$ due to the drift of the angle ϑ of each cluster toward the direction of the external field **B**. In average, the drift is equal to $-\frac{\sin\vartheta}{\tau_r}t_c$. Then, at the condition $\nu\tau_r \gg 1$, we get

$$i_{sus} = \frac{1}{2}\int_0^{\pi} \cos\left(\vartheta - \frac{\sin\vartheta}{\nu\tau_r}\right)\sin\vartheta d\vartheta \cong \frac{1}{2\nu\tau_r}\int_0^{\pi}\sin^3\vartheta d\vartheta$$
$$= \frac{2}{3\nu\tau_r} \ll 1. \quad (20)$$

From (12), $\tau_r \propto 1/B$, so the magnetization of a strongly flocculating suspension is weak and linear with B.

[41] As follows from (20), the collisions become efficient if the relaxation time τ_r exceeds the average time $t_c = 1/\nu$ between the collisions. From here, the criterion of efficiency of the collisions is the inequality $\nu\tau_r > 1$, or taking into account (12) and (15)

$$\nu\tau_r = \frac{\gamma c_0}{I_n B}\left(\frac{r}{r_m}\right)^3 \Delta\rho g r \bar{n}^{3/2} > 1. \quad (21)$$

With help of (A8) and (6), the critical depth $x_{cr}(r)$, is defined as the root of the equation:

$$\frac{\gamma c_0}{I_n B}\left(\frac{r}{r_m}\right)^3 \Delta\rho g r\left[1.3 + \frac{2.1}{4}\frac{c_0 x_{cr}}{r} + \frac{3.15}{16}\left(\frac{c_0 x_{cr}}{r}\right)^2\right]^{3/2} = 1. \quad (22)$$

Diagrams (x_{cr}, r) for $\gamma = 1.5$, $B = 50$ μT, $r_m = 0.5$ μm and different c_0 are presented in Figure 8. The region above each line corresponds to the depths x where the collisions substantially reduce the magnetization of the suspension. Naturally,

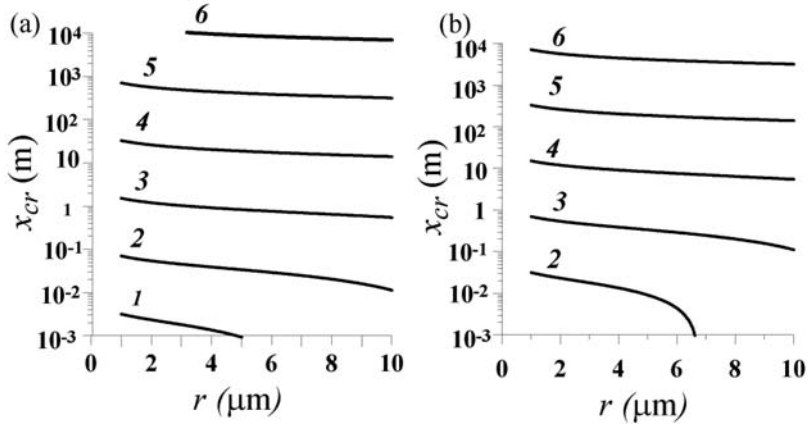

Figure 8. Critical depth x_{cr} as a function of grain size r at sticking coefficient $\beta = 1$. Diagrams (x_{cr}, r) at (a) $I_n = 100$ kA/m and (b) $I_n = 10$ kA/m. The lines on the diagrams correspond to the solutions of equation (22). Different curves represent different concentrations c_0 of the settling material on the surface of a basin: curve 1, $c_0 = 10^{-2}$; curve 2, $c_0 = 10^{-3}$; curve 3, $c_0 = 10^{-4}$; curve 4, $c_0 = 10^{-5}$; curve 5, $c_0 = 10^{-6}$; curve 6, $c_0 = 10^{-7}$.

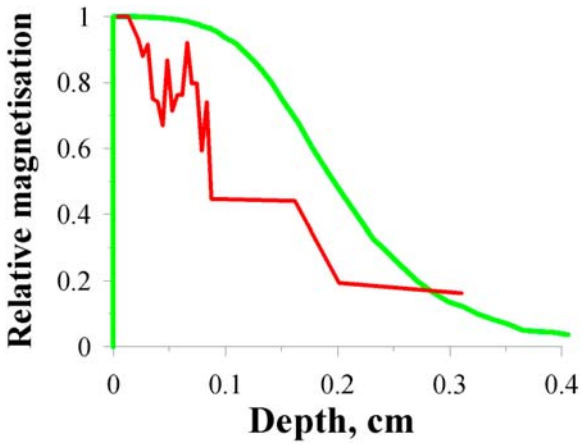

Figure 9. Variations in i_{sus} with the depth x at I_n = 10 kA/m, c_0 = 1%, and $r = r_m$ = 1 μm as computed by the numerical modeling at c_{mag} = 5% (red line). The green line shows the same curve but obtained in the approximation of mean cluster. In both cases the sticking coefficient β = 1.

the critical depth x_{cr} sharply increases with a decrease c_0 and I_n. For typical laboratory redeposition experiments, when concentrations $c_0 \sim (0.1–1)$ %, the flocculation effectively decreases the magnetization intensity of suspension already in the very top layer, even for the highly magnetic fine material with I_n = 100 kA/m (Figure 8a). But for a low concentration of the solid phase, when $c_0 \sim (10^{-6}–10^{-5})$ which is common for the sedimentation in lakes or shallow seas, the flocculation becomes effective below the depths of order (10–100) m only. For deep oceanic zones with very low rate of sedimentation when $c_0 \sim (10^{-8}–10^{-9})$, the interval between collisions t_c exceeds τ_r. Consequently, the inequality $\nu\tau_r > 1$ is never accomplished.

[42] We remind the reader that the diagrams in Figure 8 were obtained under the most favorable conditions for the flocculation process suggesting high efficiency of collisions combined with high intensity of the randomization. Formally, it means that β = 1 and D ≈ 1. Providing that these conditions are kept, the diagrams in Figure 8 claim for the absence of flocculation at low initial concentration and not enough deep basins.

6. Numerical Modeling of the Process of Magnetization of Suspension

[43] The approximation of mean cluster certainly gives only rough quantitative predictions of space-time evolution of magnetization of suspension. A more precise view can be achieved by a development of the numerical scheme used above to compute the flocculation process (Figures 3 and 4). For this, the CCA model, including Brownian motion, Van der Waals forces and Stokes settling velocity was supplied with the postulate that each collision randomizes the magnetic moments of the colliding clusters. The randomization was programmed exactly in the same manner as it was done for the mean cluster approximation described in section 5. In other words, each collision leads to a random rotation of $\mathbf{m}_{cl}$ by the angle $\Delta\vartheta$ with the equal probability within the interval $-D < \Delta\vartheta < D$ around the last value of the polar angle ϑ. The orientation of a magnetic cluster (particle) while setting in the external field is described by the well-known solution to (1),

$$tg(\vartheta/2) = tg(\vartheta_0/2)\exp(-t/\tau_r), \qquad (23)$$

where t is time that has elapsed from the moment of the last collision of the cluster with a particle or another cluster; ϑ_0 is the polar angle, assigned to $\mathbf{m}_{cl}$ after the last collision occurred. Recall that (23) is valid only between collisions.

[44] The plots shown in Figure 9 were computed from the results obtained in full similarity with those shown in Figure 4 except for the additional monitoring of the magnetic moments of particles and clusters. For this, there were randomly distributed 2 or 4% of magnetic grains with $r_m = r$ = 1 μm carrying the remanent magnetization I_n = 10 kA/m. The numerically computed magnetization (redline) demonstrates the sharp decrease in the magnetization intensity with depth x from the very beginning, when clusters are not formed yet to hinder the process of orientation of $\mathbf{m}_{cl}$ along $\mathbf{B}$. This feature is in clear contrast to what was found by the mean cluster algorithm (the green line). The reason for this discrepancy is that after a collision of two clusters, on the condition that each of them contains magnetic particles, the total magnetic moment $\mathbf{m}_{cl}$ of the newly formed cluster is always less than the arithmetic sum of its constituents. Hence, each collision of two clusters containing magnetic grains, decreases the net magnetic moment of the suspension even at $\nu\tau_r < 1$.

7. Discussion

[45] Our models show that the space-time evolution of magnetization of suspension is determined by the six parameters: c_0, r, r_m, D, I_n, and B. In

addition, there is another important parameter, namely, the sticking coefficient of collisions β, which was not included in our analysis up to now. This correction can be disregarded if the deposition occurs in saline water. But in distilled or low-salinity water the probability of sticking can be very low due to the repulsion of particles so the efficiency of the flocculation mechanism will be suppressed by approximately a factor of $1/\beta$ [*Fuchs*, 1964]. A strong dependence of DRM on deposition conditions and especially on water salinity is well documented [*Shcherbakova*, 1986; *Bol'shakov and Kurazhkovskii*, 1989; *van Vreumingen*, 1993; *Katari and Tauxe*, 2000; *Tauxe et al.*, 2006]. In particular, the critical depths x_{cr} in Figure 8 must be multiplied by about $1/\beta$. Correspondingly, at low salinities, the lines (x_{cr}, r) in the diagrams must be shifted up, leaving the possibility of absence of flocks even at relatively high sedimentation rate. This could occur in lakes where mineralization is very low.

[46] In nature, flocculation could be caused by other mechanisms than Brownian motion. It can be triggered also by small-scale turbulence of the hydrodynamic flow, organic matter which increases the sticking coefficient, etc. Furthermore, the upper layer of sediment is often subjected to intensive mixing [*Roberts and Winklhofer*, 2004]. As *Tauxe et al.* [2006] suggested, the stirring energy can be sufficient to fluidize the material of the very top layer so that floccules will occasionally experience uplift with subsequent "redeposition" on the denser bottom. If this process is really intensive, and the concentration of the floating clusters is high enough, collisions between them might effectively influence the resulting DRM, independent of sedimentation rate. So, we do not advocate that flocs are necessarily absent in slowly deposited sediments or in basins with low salinity. This question is purely the matter of direct observations. Actually, the existence of floccules of different sizes in marine sediments is well demonstrated by direct observations (references are given by *van Vreumingen* [1993] and *Tauxe et al.* [2006]).

[47] Such a multiparametric dependence of the intensity of I_{sus} on the deposition conditions does not impede determinations of relative paleofield intensity (providing that necessary precautions are taken) but makes senseless determinations of absolute paleomagnetic intensity by the method of redeposition in view of impossibility to reproduce all natural parameters with the necessary accuracy in laboratory experiments. Similar considerations were advocated by *Dunlop and Ozdemir* [1997].

[48] To this end, the outcome of our analysis can be summarized as follows. For the very first moment, when a well dispersed sedimentary material just appears on the water surface, it almost immediately becomes aligned along **B** in accordance with the classical Nagata's model. What follows next depends on the degree of dilution of the suspension, value of the sticking coefficient, depth of the basin. If the dilution (rate of accumulation) is low, the depth of the basin is not big and/or the sticking coefficient is small, this high magnetization may survive all the way down to the basin bottom. In the opposite case, the magnetization of suspension decreases with depth due to the onset of frequent collisions between the floccules (in accordance with the flocculation model). Curiously, in the latter case the process of "acquisition of DRM" during sedimentation can be rather characterized as the process of decay of the initially acquired "too strong" magnetization. In other words, there is no a real contradiction between the Nagata's and flocculation models; both are just extreme ends of the same alignment mechanism.

[49] This scenario is supported by experimental results by *van Vreumingen* [1993] who studied the time evolution of magnetization intensity of suspensions containing mainly nonmagnetic grains mixed with small amount of magnetite or maghemite submicron particles. The volume concentration of the solid phase was c_0 = 1%–2%, the magnetic particles comprised only ≈0.1% of c_0, and, importantly, the magnetization was measured in the presence of the external field $B = 47\ \mu$T. Under these experimental conditions, the magnetization measured only 5 s after the start of the settling, was close to the saturation magnetization I_{sat} if the experiments were done at low and intermediate salinities, less than (3–4) g/l. At the higher salinities the intensity of the magnetization of suspensions drastically decreases below I_{sat}. Noteworthy, the magnetization intensity quickly decays with time at all salinities. Thus, I_{sus} decreased by (2–4) times 10 min after the start of the deposition at low salinities <1 g/l and the drop was even more at salinities >(3–4) g/l.

[50] Qualitatively, these facts fit well with the flocculation model. Indeed, at zero and low salinities the repulsive forces are strong and the agglomeration is suppressed. Thus, magnetic moments of grains and clusters have enough time for the alignment along **B** giving rise to higher I_{sus}, though a certain decrease of I_{sus} with time shows that some degree of clustering still takes place. On the other hand, at higher salinities the collisions are so inten-

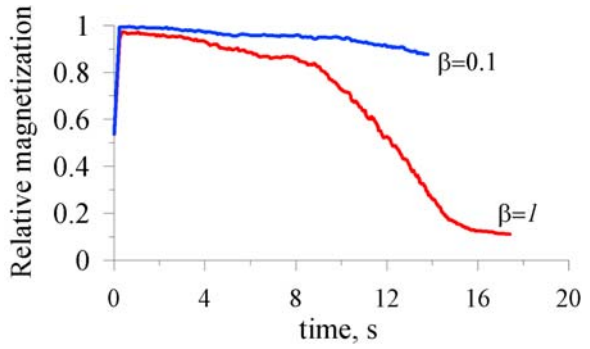

Figure 10. Computer modeling of *van Vreumingen*'s [1993] experiments. Variations in the normalized net magnetization of the suspension settling in a cube 1.53 cm in depth versus time. I_n = 10 kA/m. The red curve corresponds to the sticking coefficient β = 1, and the blue one corresponds to the sticking coefficient β = 0.1.

sive that already in 5 s after the start of the settling, the magnetization intensity of suspensions drops to the level which is a few times less than I_{sat}.

[51] We attempted to carry out a computer modeling of the experiments by *van Vreumingen* [1993] using the same CCA model with gravitational settling. For this, N = 70000 particles with the initial volume concentration 2% were uniformly distributed over a narrow long parallelepiped with width A = 31 μm and height A^* = 1.53 cm. Recall that the periodic conditions were imposed on the walls of the parallelepiped. The sizes of nonmagnetic and magnetic grains were taken as r = 1 μm and r_m = 0.5 μm, respectively. The number of magnetic grains was taken as higher as $N_m = 0.02N$ which considerably exceeds the percentage of the magnetic fraction in the experiments performed by *van Vreumingen* [1993]. However, this discrepancy seems to be inevitable to the necessity to have enough magnetic grains in the numerical ensemble for statistical treatment of the results.

[52] First, the case of high salinities was simulated when the sticking coefficient is presumably = 1. The red curve in Figure 10 shows the normalized to I_{sat} net magnetization of the parallelepiped $i(t) = \sum_{j=1}^{N_m} \cos \vartheta_j$ as function of time. Here the summation is done over all magnetic grains in the ensemble. As expected, the magnetization quickly increases from zero to almost saturation value in less than a second. Then it gradually decreases with time increase until between 8 and 16 s the decrease becomes much steeper. At t > 20 s the drop in $i(t)$ almost ceases and the process reaches an asymptotic regime. As is seen, the behavior of the magnetization intensity in this numerical experiment is in a reasonable agreement with the experimental data by *van Vreumingen* [1993] for the case of high salinities, when the magnetization intensity drastically fall below the saturation value already 5 s after the start of the settling process. The difference in time of the onset of the drop between the depositional and numerical experiments is not significant accounting for the number of approximations assumed in the numerical computations.

[53] The second numerical experiment, aimed to imitate low-salinity conditions, was done with the sticking coefficient β = 0.1. Naturally, it showed much slower decay of $i_{sus}(t)$ so that at t = 5 s almost no decrease of the magnetization intensity was observed (blue curve). Again, this result fits well to the experiments with low salinities when i_{sus} only insignificantly decreases for the first minutes.

[54] The key element of the flocculation model is the suggestion that each collision leads to a certain randomization of magnetic moments of the colliding clusters. For a first glance, a suitable agent capable to disorient $\mathbf{m}_{cl}$ is the thermal Brownian motion energy. However, remembering that the Zeeman energy of magnetic grains in the Earth's magnetic field usually considerably exceeds the thermal one, the Brownian motion should be rule out as an effective cause of the randomization. But the kinetic energy E_{kin} of the gravitational settling of a cluster can carry the needed energy. Indeed, taking into account the expression (5) for the settling velocity and accepting for simplicity the fractal dimension of clusters d = 2, we obtain

$$E_{kin} = \frac{4\pi\Delta\rho r^3}{3} u^2/2 = \frac{8\pi r^7 \Delta\rho^3 g^3 n^2}{243\eta^2}, \qquad (24)$$

At grain sizes r > 1 μm and the number of grains in the cluster n > 10 this value considerably exceeds k_BT. Thus, this type of collision, when a big settling cluster picks up the smaller ones, may provide sufficient randomization energy.

[55] Perturbations of cluster orientation can be also caused by the hydrodynamic torques developing during collisions. Due to these torques, clusters will rotate in space in order to find a new balance between gravitational, magnetic and hydrodynamic torques.

[56] But most plausible and effective cause of the randomization, on our opinion, is the restructuring of clusters. The restructuring is a tool to decrease the total energy of a cluster when its particles find

new positions with deeper van der Waals potential wells. Note that the energies of these wells range from 1 to 1000 k_BT [*Derjaguin*, 1989; *West et al.*, 1994], so they are much more powerful than the thermal and Zeeman's energies. As *Meakin and Jullien* [1988, p. 246] pointed out, "one of the characteristic properties of fractal aggregates is their susceptibility to distorting and/or fragmentation as a result of thermal fluctuations and/or external fields… One way in which the fractal dimensionality of aggregates might increase is via structural reorganization after pairs of clusters have moved into contact with each other but before strong bonding has occurred." In this sense, the restructuring means the reorientation and displacement of particles inside a cluster. Both these processes lead to the consolidation of clusters and the corresponding increase in fractal dimension of aggregates. In particular, the restructuring leads to increase of the number of contact points between aggregates through rotations of the rigid clusters about the contacts.

[57] The fragmentation of clusters, the rotation and displacement of particles inside clusters can happen only on the condition that some potential wells securing the bonds are not so deep. The characteristic time of escape of a particle trapped in a potential well as a result of thermal fluctuations, is given by the well-known Kramers' formula [*Hänggi et al.*, 1990]

$$\tau = \frac{12\pi^2 r\eta}{\sqrt{E''(z_{\min})E''(z_{\max})}}\exp\left(\frac{\Delta E}{k_B T}\right). \qquad (25)$$

Here $E(z)$ is the energy function, $z_{\min}$ and $z_{\max}$ are the positions of the minimum and maximum of $E(z)$, $\Delta E = E(z_{\max}) - E(z_{\min})$ is the potential barrier. For a rough estimation let us put $E''(z_{\min}) = E''(z_{\max}) \sim \frac{\Delta E}{\alpha^2 r^2}$, where the parameter $\alpha \ll 1$. The last inequality is conditioned by the fact that the distance $z_{\min}$ between coalescing particles is much less than their radius r. Then (25) reduces to

$$\tau \sim \frac{12\pi 2r^3\eta\alpha^2}{\Delta E}\exp\left(\frac{\Delta E}{k_B T}\right). \qquad (26)$$

Simple calculations show that at $\Delta E \sim 10\ k_BT$, $r \sim 1\ \mu$m and $\alpha \sim 0.1$, the characteristic time τ is less than 10 s. Hence, relatively low potential barriers with $\Delta E < (10–15)\ k_BT$ can be easily surmounted giving way to the restructuring processes.

[58] In our model, when a cluster or particle touches the water-sediment interface, it experiences a random rotation following by the fixation of the orientation and positions of the particles. These random rotations lead to the drop of $I_{sus}(H)$ in the suspension layer adjacent to the water/sediment interface by a value ΔI_{sus}. Hence, the "slurry" acquires DRM = $I_{sus}(H) - \Delta I_{sus}$. In other words, DRM inherits the magnetization of the deepest layer of the suspension with a correction for the possible intensity loss due to the random rotation of $\mathbf{m}_{cl}$ when clusters touch the water/sediment surface.

[59] One can imagine that the intensity loss is so tremendous that the processes of settling and flocculation are simply irrelevant to the formation of I_{rd}. If this were the case, the pDRM would constitute the main part of I_{rd}. But the direct monitoring of the time evolution of intensity of I_{sus} and DRM reported by *van Vreumingen* [1993] clearly show that it is not true and DRM inherits the magnetization of flocculating suspension. The same conclusions can be drawn from the experiments carried out by *Barton et al.* [1980], *Verosub* [1977], *Payne and Verosub* [1982], *Katari et al.* [2000], and *Tauxe et al.* [2006] who found that the intensity of pDRM is insignificant in comparison with the intensity of DRM as long as there is no agitation of the settled slurry.

[60] The common physical explanation for the phenomenon of pDRM is that some magnetic grains are free to rotate to some extent after the deposition. It is certainly plausible as magnetite grains usually are finer than the nonmagnetic ones and for this reason they often have only one contact with the host grain. Besides, due to the fractal structure of clusters deposited on the water/sediment interface, a huge number of pores are present in the top layer of sediment. Consequently, it is not a rare case that a grain has only one neighbor; thus, it can easily rotate around the contact points under the action of an external force. In addition, rotations are also possible if there exist not just one, but two contact points.

[61] These rotations allow for the rapid elastic deformations which are a part of rheological properties of wet sediments [*Rieke and Chilingarian*, 1974; *Nichiporenko et al.*, 1974]. Besides, there exist the so-called slow elastic deformations developing on the time scale of (100–1000) s due to reversible displacements (slipping) of contact points along the contacting surfaces.

[62] Judging on the existence of the elastic deformations, a simple physical scheme of pDRM acquisition can be proposed as follows. As far as the external magnetic field is applied, the induced

magnetization of the slurry is caused by the elastic deformations. The intensity of the induced magnetization is proportional to the amplitude of the deformations which are determined by the balance between the magnetic torque and shear strength of the sediment matrix [*Shcherbakov and Shcherbakova*, 1987]. However, due to the reversibility of the elastic deformations, this magnetization is unstable and quickly decays after the field is switched off. Such decay of the remanent magnetization in slurries on the time scale of (100–1000) s was indeed observed experimentally by *Tucker* [1980] and *Heslop et al.* [2006].

[63] The situation changes radically, if the sediment, subjected to an external field, experiences the compaction and consolidation while sinking in deeper layers due to continuous sedimentation. The compaction and consolidation are accompanied by the restructuring of the sediment and generation of new contact points which may lock rotations of grains. Hence, the induced magnetization can be frozen forming now the stable in time pDRM. In particular, the well-known redeposition experiments by *Lovlie* [1976] can be explained suggesting that the structure of some samples was so loose that the induced magnetization (which was aligned of course along the applied field without respect to its direction) was frozen only at the depths more than 10 cm below the marker horizon where the change of the declination of the applied field occurred.

[64] As declared in the introduction, the ultimate aim of this study is to estimate the role of flocculation for the formation of sediment magnetization. The qualitative prediction of the model is that, when flocculation is absent, DRM is close to the saturation, while, when flocculation is intensive, DRM is far from the saturation. In other words, at high sedimentation rate the intensity of magnetization should be lower than at low sedimentation rate, provided that the mineralization is the same. From this, one can try to estimate the role of flocculation for the formation of NRM. This estimate starts from the assumption that the ratio NRM/SIRM, where SIRM the saturation remanent magnetization, is inverse proportional to the intensity of flocculation. Unfortunately, we are not aware of any systematic studies of the NRM/SIRM ratio on global scale up to now. The possible outcome of such the study (when it will be done) may be shortly described as follows.

[65] If the NRM/SIRM ratio occurs to be systematically higher for sediments with high sedimentation rate (or lower mineralization), this would strongly support the flocculation model as well as the concept that NRM inherits much of the DRM. However, if NRM/SIRM occurs to be globally the same, despite different sedimentation rates, this could have two possible reasons. Either flocculation is effective everywhere, despite low sedimentation rate and low mineralization, or the DRM contributes only little to the NRM, which is mostly generated by pDRM processes. The first subcase seems to be more likely, because the presence of flocs is well documented in different basins. The second subcase would imply that all memory about the primary DRM is lost in course of postsedimentary processes. In any case, this emphasizes the importance of measuring absolute values of rock magnetic parameters and critical ratios such as NRM/ARM and NRM/SIRM. Also microscopic observations of the structure of topmost layer of undestroyed sediment columns will be of major value. Such data will provide good evidence pro or contra the central role of flocculation in the formation of the natural remanent magnetization of sediments.

8. Conclusions

[66] At high sedimentation rate the flocculation is an important factor that strongly decreases the intensity of the sedimentary magnetization. The only exception may be the sedimentation in very low mineralized water, when the probability of aggregation of particles is very low. Then the sedimentary magnetization may saturate already in the Earth's magnetic field.

[67] Under natural conditions, relatively high sedimentation rate is common for deepwater lakes and coastal sea basins where the flocculation process may effectively decrease the sedimentary magnetization. For pelagic oceanic regions the sedimentation rate is small and the flocculation hardly influences the intensity of sedimentary magnetization there until other factors like turbulence and biotic processes come into play.

[68] Large divergences between numerous experimental results of different authors can be at least partly explained in terms of different intensity of flocculation during the settling.

[69] To understand mechanisms of formation of DRM and pDRM, it is not enough to carry out experiments with the remanent magnetization of deposited sediments only. In order to comprehend the physics of DRM and pDRM acquisition, it is necessary to perform continuous monitoring of

both induced and remanent magnetizations of suspensions in the processes of their settling and compaction.

Appendix A

[70] Following *Jullien* [1987], the Smoluchowski coagulation equation (continuous version) can be written as follows:

$$\frac{\partial N(n,t)}{\partial t} = -N(n,t)\int_0^\infty \gamma(n,k)N(k,t)dk + 1/2\int_0^n \gamma(n-k,k)N(n-k,t)N(k,t)dk. \quad \text{(A1)}$$

Here γ is the collision γ rate, $N(n, t)$ is the density of clusters (number per unit volume) containing n particles at the time moment t, $N(t) = \sum_n N(n, t)$ is the density of all clusters. The density of all particles, regardless of whether they belong to a cluster or not is $N_0 = \sum_m nN(n, t)$. The average number of particles in a cluster is $\overline{n}(t) = \sum_m nN(n, t)/N(t) = N_0/N(t)$. At γ = const, equation (A1) has an analytical solution with $\overline{n}(t) - \propto t$.

[71] To account for the gravitational settling, one should replace the partial derivative in the left-hand side of (A1) by the total derivative and add a term describing the gravitational coagulation:

$$\frac{\partial f(n,t,x)}{\partial t} + u(n)\frac{\partial f(n,t,x)}{\partial x} = -f(n,t,x)N_0\left[\int_0^\infty \gamma(n,k)f(k,t,x)dk + \frac{1}{2}\int_0^n \gamma(n-k,k)f(n-k,t,x)f(k,t,x)dk\right]. \quad \text{(A2)}$$

Here $f(n, t, x) = N(n, t, x)/N_0$ is the density of clusters normalized to N_0 and $u(n) = 2\Delta\rho g r^2 n^{(d-1)/d}/9\eta$ is the settling velocity of a cluster. The collision rate is $\gamma(n, k) = \gamma_{br}(n, k) + \gamma_{gr}(n, k)$, where $\gamma_{br}(n, k) = \frac{2k_BT\left[R_g(n)+R_g(k)\right]^2}{3\eta R_g(n)R_g(k)}$ is the collision rate due to the Brownian motion obtained by a simple generalization of (3) and

$$\gamma_{gr}(n,k) = 2\pi\Delta\rho g r^4\left(n^{1/d}+k^{1/d}\right)^2\left|n^{(d-1)/d}-k^{(d-1)/d}\right|/9\eta \quad \text{(A3)}$$

is the gravitational collision rate obtained by a generalization of (4).

[72] An isolated grain settles onto the bottom in the time interval $t_f = H/u(r)$. Taking the basin depth $H \sim (10–10^5)$ cm, $r \sim 1$ μm, simple calculations at $R_g = r$ with help of (5) show that t_f can hardly exceed a few years. Agglomerates settle even quicker conglomerates fall down even quicker, one can conclude that t_f is usually much smaller than the characteristic time of variations of natural conditions of deposition. In this quasi-stationary case (A3) reduces to

$$u(n)\frac{df(n,x)}{dx} = N_0\left[-f(n,x)\int_0^\infty \gamma(n,k)f(k,x)dk + \frac{1}{2}\int_0^n \gamma(n-k,k)f(n-k,x)f(k,x)dk\right] \quad \text{(A4)}$$

with the initial condition $f(n, 0) = f_0(n)$. Noteworthy, that the solution of (A4) has the invariant

$$U = \int_0^\infty u(n)nf(n,x)dn = \text{const}, \quad \text{(A5)}$$

which manifests the constancy of the number of particles crossing any plane x = const per unit time. As far as $N_0(4\pi/3)r^3 = c_0$, where $\tilde{n}_0$ is the relative volume concentration of material on the basin surface, (A4) transforms to:

$$\frac{df(n,X)}{dX} = \frac{1}{n^{(d-1)/d}}\left[-f(n,X)\int_0^\infty s(n,k)f(k,X)dk + \frac{1}{2}\int_0^n s(n-k,k)f(n-k,X)f(k,X)dk\right], \quad \text{(A6)}$$

where the reduced collision rate

$$s(n,k) = \left(n^{1/d}+k^{1/d}\right)^2\left[\frac{a}{(nk)^{1/d}} + \left|n^{(d-1)/d}-k^{(d-1)/d}\right|\right] \quad \text{(A7)}$$

and the dimensionless coordinate

$$X = \frac{3c_0x}{4r}. \quad \text{(A8)}$$

[73] As is evident from the structure of (A6) and (A7), the coefficient

$$a = 3k_BT/\pi r^4\Delta\rho g \quad \text{(A9)}$$

is the only dimensionless parameter forming the shape of distribution function (d. f.) $f(n, X)$. Physically, it characterizes the predominance of Brownian ($a > 1$) or gravitational ($a < 1$) coagulation types on the initial stage of settling (when the flocculation is well developed, the gravitational coagulation takes over anyway). At $r = (0.1–10)$ μm the parameter a varies from 10^4 to 10^{-4}. Accordingly, the domination of Brownian or gravitational coagulation happens at $r < 1$ μm or $r > 1$ μm, respectively.

Acknowledgments

[74] The work is supported by the Russian Fund of Basic Researches, grant 06-05-64585. Thoughtful and constructive reviews by Jean-Pierre Valet and Michael Winklhofer as well as the remarks from the theme editor, Bruce Moskowitz, largely improved the paper.

References

Barton, C. E., M. W. McElhinny, and D. J. Edwards (1980), Laboratory studies of depositional DRM, *Geophys. J. R. Astron. Soc.*, *61*, 355–377.

Bol'shakov, A. S., and A. Y. Kurazhkovskii (1989), Ionic composition of water and magnetization of sediments (in Russian), *Izv. Akad. Nauk SSSR, Ser. Fiz.*, *5*, 118–126.

Carter-Stiglitz, B., J.-P. Valet, and M. LeGoff (2006), Constraints on the acquisition of remanent magnetization in fine-grained sediments imposed by redeposition experiments, *Earth Planet. Sci. Lett.*, *245*, 427–437, doi:10.1016/j.epsl.2006.03.002.

Chermous, M. A., and V. P. Shcherbakov (1980), Fluid-dynamic implication for acquisition of sedimentary magnetization (in Russian), *lzv. Acad. Nauk SSSR Earth Phys.*, *1*, 120–124.

Collinson, D. W. (1965), Depositional remanent magnetization in sediments, *J. Geophys. Res.*, *70*(18), 4663–4668, doi:10.1029/JZ070i018p04663.

Derjaguin, B. V. (1989), *Theory of Stability of Colloids and Thin Films*, 258 pp., Consult. Bur., New York.

Dunlop, D. J., and O. Ozdemir (1997), *Rock Magnetism: Fundamentals and Frontiers*, Cambridge Univ. Press, Cambridge, U. K.

Fuchs, N. A. (1964), *The Mechanics of Aerosols*, Pergamon Press, Oxford, U. K.

Hänggi, P., P. Talkner, and M. Borkovec (1990), Reaction-rate theory: Fifty years after Kramers, *Rev. Mod. Phys.*, *62*, 251–341, doi:10.1103/RevModPhys.62.251.

Heslop, D. (2007), Are hydrodynamic shape effects important when modelling the formation of depositional remanent magnetization?, *Geophys. J. Int.*, *171*(3), 1029–1035.

Heslop, D., A. Witt, T. Kleiner, and K. Fabian (2006), The role of magnetostatic interactions in sediment suspensions, *Geophys. J. Int.*, *165*, 775–785.

Johnson, E. A., T. Murphy, and O. W. Torreson (1948), Prehistory of the Earth's magnetic field, *Terr. Magn. Atmos. Electr.*, *53*, 349–372, doi:10.1029/TE053i004p00349.

Jullien, R. (1987), Fractal aggregates, *Comments Condens. Matter Phys.*, *13*(4), 177–205.

Katari, K., and L. Tauxe (2000), Effects of surface chemistry and flocculation on the intensity of magnetization in redeposited sediments, *Earth Planet. Sci. Lett.*, *181*, 489–496, doi:10.1016/S0012-821X(00)00226-0.

Katari, K., L. Tauxe, and J. King (2000), A reassessment of post depositional remanent magnetism: preliminary experiments with natural sediments, *Earth Planet. Sci. Lett.*, *183*, 147–160.

Kent, D. V. (1973), Post-depositional remanent magnetization in deep-sea sediment, *Nature*, *246*, 32–34, doi:10.1038/246032a0.

Kolb, M., R. Botet, and R. Jullien (1983), Scaling of kinetically growing clusters, *Phys. Rev. Lett.*, *51*, 1123, doi:10.1103/PhysRevLett.51.1123.

Lovlie, R. (1976), The intensity of post-depositional remanence acquired in some marine sediments deposited during a reversal of the external magnetic field, *Earth Planet. Sci. Lett.*, *30*, 209–214.

Meakin, P. (1983), Formation of fractal clusters and networks by irreversible diffusion-limited aggregation, *Phys. Rev. Lett.*, *51*, 1119–1122, doi:10.1103/PhysRevLett.51.1119.

Meakin, P., and R. Jullien (1983), The effects of restructuring on the geometry of clusters formed by diffusion-limited, ballistic, and reaction-limited cluster–cluster aggregation, *J. Chem. Phys.*, *89*, 246, doi:10.1063/1.455517.

Mitra, R., and L. Tauxe (2009), Full vector model for magnetization in sediments, *Earth Planet. Sci. Lett.*, *286*, 535–545, doi:10.1016/j.epsl.2009.07.019.

Nagata, T. (1961), *Rock-Magnetism*, 348 pp., Maruzen, Tokyo.

Nichiporenko, S. P., N. N. Kruglizkyi, A. A. Panasevich, and V. V. Khilko (1974), *Physiko-chimitcheskaya mechanika dispersnich mineralov* (in Russian), 246 pp., Nauk. Dumka, Kiev.

Payne, M., and K. Verosub (1982), The acquisition of post-depositional detrital remanent magnetization in a variety of natural sediments, *Geophys. J. R. Astron. Soc.*, *68*, 625–642.

Rieke, H. H., and G. V. Chilingarian (1974), *Compaction of Argillaceous Sediments*, 1st ed., Elsevier, New York.

Roberts, A., and M. Winklhofer (2004), Why are geomagnetic excursion not always recorded in sediments? Constraints from post-depositional remanent magnetization lock-in modeling, *Earth Planet. Sci. Lett.*, *227*, 345–359, doi:10.1016/j.epsl.2004.07.040.

Shcherbakov, V., and V. Shcherbakova (1983), On the theory of depositional remanent magnetization in sedimentary rocks, *Geophys. Surv.*, *5*, 369–380, doi:10.1007/BF01453987.

Shcherbakov, V. P., and V. V. Shcherbakova (1987), On the physics of acquisition post-depositional remanent magnetization, *Phys. Earth Planet. Inter.*, *46*, 64–70.

Shcherbakov, V. P., and N. K. Sycheva (2008), Flocculation mechanism of the acquisition of remanent magnetization by sedimentary rocks, *Izv. Phys. Solid Earth*, *44*(10), 804–815, doi:10.1134/S106935130810008X.

Shcherbakov, V. P., and N. K. Sycheva (2009), Numerical modeling of magnetization of a precipitating rock suspension, *Izv. Phys. Solid Earth*, *45*(1), 47–56, doi:10.1134/S1069351309010078.

Shcherbakova, V. V. (1986), Influence of the redeposition technique on remanence characteristics of redeposited samples (in Russian), in *Fine Structure of the Geomagnetic Field*, pp. 123–128, Inst. of Phys. of the Earth, Moscow.

Shive, P. N. (1985), Alignment of magnetic grains in fluids, *Earth Planet. Sci. Lett.*, *72*, 117–124, doi:10.1016/0012-821X(85)90121-9.

Stacey, F. (1972), On the role of Brownian motion in the control of detrital remanent magnetization of sediments, *Pure Appl. Geophys.*, *98*, 139–145, doi:10.1007/BF00875588.

Tauxe, L., and D. V. Kent (1984), Properties of a detrital remanence carried by hematite from study of modern river deposits and laboratory redeposition experiments, *Geophys. J. R. Astron. Soc.*, *77*, 543–561.

Tauxe, L., J. L. Steindorf, and A. Harris (2006), Depositional remanent magnetization: Toward an improved theoretical and experimental foundation, *Earth Planet. Sci. Lett.*, *244*, 515–529, doi:10.1016/j.epsl.2006.02.003.

Tucker, P. (1980), Stirred remanent magnetization: A laboratory analogue of postdepositional realignment, *J. Geophys.*, *48*, 153–157.

van Vreumingen, M. J. (1993), The magnetization intensity of some artificial suspensions while flocculating in a magnetic field, *Geophys. J. Int.*, *114*, 601–606, doi:10.1111/j.1365-246X.1993.tb06990.x.

Verosub, K. (1977), Depositional and postdepositional processes in the magnetization of sediments, *Rev. Geophys.*, *15*, 129–143, doi:10.1029/RG015i002p00129.

West, A. H. L., J. R. Melrose, and R. C. Ball (1994), Computer simulations of the breakup of colloid aggregates, *Phys. Rev.*, *49*(5), 4237–4249.

Witten, T. A., and L. M. Sander (1981), Diffusion-limited aggregation, a kinetic critical phenomenon, *Phys. Rev. Lett.*, *47*, 1400, doi:10.1103/PhysRevLett.47.1400.